Kinematic Modelling for Glenohumeral Shoulder of Humanoid Robot

AHMAD TAYBA
University of Paris Saclay
LISV laboratory
10, 12 avenue de l'Europe Velizy-Villacoublay
FRANCE
ahmad.tayba@lisv.uvsq.fr

SAMR ALFAYAD
University of Paris Saclay
LISV laboratory
10, 12 avenue de l'Europe Velizy-Villacoublay
FRANCE
samer.alfayad@lisv.uvsq.fr

FETHI B. OUEZDOU
University of Paris Saclay
LISV laboratory
10, 12 avenue de l'Europe Velizy-Villacoublay
FRANCE
ouezdou@lisv.uvsq.fr

FAYCAL NAMOUN
President of BIA
Institute of Mechanical Engineering
ZA Les Noutries, 8 rue de lHautil, Conflans fin dOise
FRANCE
f.namoun@bia.fr

Abstract: This paper aims to develop the kinematic model for a hybrid structure proposed for the Glenohumeral shoulder of humanoid robot. A detailed description for the three Degree Of Freedom (DOF) model has been presented and then, a detailed geometrical model has been carried out in order to be used as a powerful tool for the optimization process.

Key–Words: Humanoid Robots, Shoulder Complex, Glenohumeral and Girdle shoulder.

1 Introduction

The development of a humanoid robot has recently received an important attention, especially when it entrusted with the task of space discovering, human save and other medical jobs. Hence, there were different ways of thinking according to the design of these robots. Some wanted to get a humanoid robot with high degree of intelligence with no caring about the morphology and human being. Other, they focused on the degree of anthropomorphism in order to emulate the motion of human for medical and rehabilitation purposes. Therefore, the design constraints grows up, due to the scarcity and lack of anatomy information about human kinematic ,and also due to mechanical, design space and manufacturing constraints.

Shoulder complex is one of the complex mechanism in human body. Therefore, an exact kinematic model that describes this mechanism is difficulty obtained. In general, it is composed from Inner and Outer joint. The Sterno-Clavicular (SC) joint occurs between the proximal end of the clavicle and the sternum. It allows a 3 DOF, Elevation and Depression, Protraction and Retraction, and axial rotation. Thus, it can be modelled as a ball and socket joint with a predefined range of motion. The Acromio-Clavicular (AC) joint exist between the acromion of the scapula and the distal end of the clavicle. All movements at this joint are passive; there is no muscle present which produce an active movement between the bones[12]. The Scapulo-Thoracic (ST) joint is a gliding joint which allows the scapula to glide over the thoracic[15][16]. Different model assumed that the ST joint can be modeled as 4 or 5 DOF [13][14]. All the presented joints are including in the inner joint of the shoulder complex and its called the Shoulder Girdle. The outer joint of the shoulder complex is called the Glenohumeral joint which occurs as a ball and socket joint between the humerus and glenoid fossa of the Scapula[12]. This large number of degree of freedom are associated with each other to offer the most mobile kinematic system in human body. The figure 1 present the different bones and joint for the shoulder complex.

Since decades, many researches have been invested to get a kinematic model for the Shoulder Complex to use it even for humanoid robot or other medical devices. HRP4[1], Asimo[2], H7[3], Qrio[9],

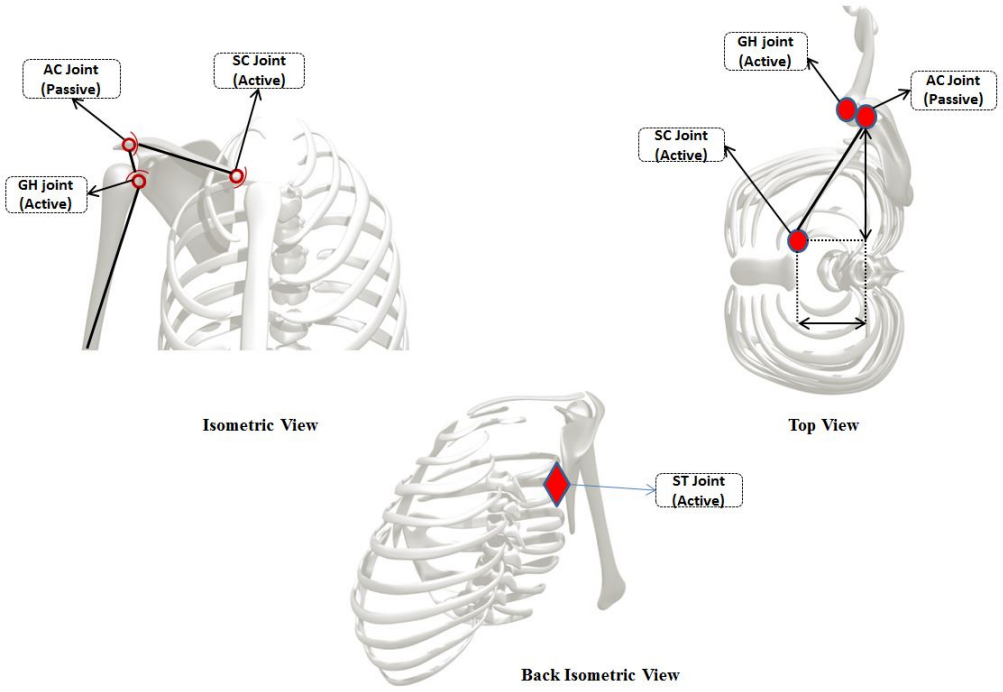

Figure 1: Bones and joints of the Shoulder Complex[12]

Wabian[10], and CB[11] are using a simple serial mechanism to model the shoulder glenohumeral joint to provide more simplicity in the manufacturing process. However , the serial configuration suffer from heavy weight and bulky mechanism since that each actuator has to support the weight of its followers. Nevertheless, this configuration can be easily modelled using the conventional method for direct or inverse geometrical, kinematic and dynamic models, and therefore the way to control such mechanism become more simple and easy. As far as we know, a small number of biped robot use a parallel mechanism for the shoulder, due to the limited range of motion that can be offered such mechanism. however, and thanks to the rigidity of paralell mechanisms, it can be an ideal solution for shoulder kinematic to ensure the stability and the rigidty during motion. OKADA et al. have introduces the mechanical softness in the design of shoulder :"The mehanical Softness include such requirement as human-like high mobility and human-like sensitive compliance". [8]. Nevertheless they use a parallel mechanism , its actuators use a large space from the chest to locate the actuators preventing the ability to develop an active torso inside the robot.

In this paper, we will present the kinematic structure proposed for the first part of the shoulder complex (Glenohumeral). Our proposed solution consist of using a hybrid mechanism which combine the benefit of serial (large range of motion) and parallel mechanism (stability and rigidity). This mechanism should be integrated to the underdevelopment humanoid robot HYDROïD [6][7][17]. The HYDROïD will have the size of 1.6 m and a weight of almost 120 Kg and has 1.2 m/s as a nominal speed. All the HYDROïD body joint are actuated hydraulically [18],while it head is actuated electrically [19].

The first part will describe the proposed kinematic structure to get the three DOF of the glenohumeral shoulder, then, a generalized analytical model for the inverse geometrical model will be presented in order to get a powerful tool for the optimization process such as design, shape and geometrical optimization. In addition to this, this model will be used as a feedback for the control algorithm of such mechanism.

2 Structure Description

According to the anatomy study, the outer joint of the shoulder complex is called the Shoulder Glenohumeral joint (SG) which occurs as a ball and socket joint between the humerus and glenoid fossa of the Scapula. Therefore, it can be modeled as a spherical joint with 3 intersecting axes.

The hybrid solution proposed for the SG joint of HYDROD is depicted in Figure 2. It consists of a 3-DoF mechanism that has 17 joints arranged in three kinematic chains leading to two independent closed loops. Starting with a serial chain with a rotary joint allows us to have a large range of motion around the

pitch axis, reaching almost $180°$. For the 2 other DOF , rotation arround Roll and Yaw axis are obtained from 2 linear actuators (A2 and A3) in the input to produce a large motion at the output and to decrease the singularity positions. Each of linear actuator are located in 3D space between 2 spherical joints (A and D), (B and E), F and G . The Whole description for the choice of such mechanism can be found in the following reference[5].

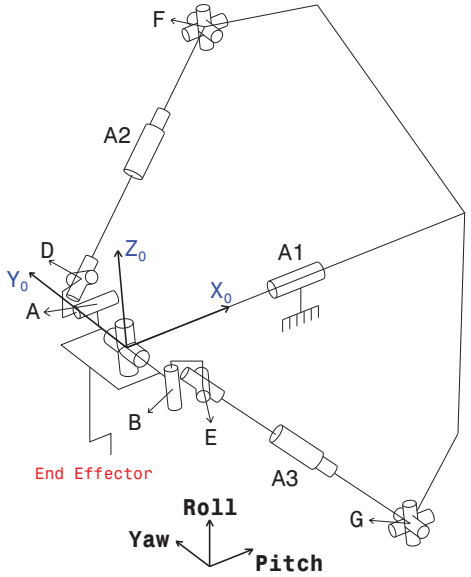

Figure 2: General Kinematic Model for Glenohumeral Shoulder

3 Parameter Description

The parameter description based on the Khalil et al. notation [4] of the new solution is given in Table 1, Where the main parameters are defined as follow: α_j is the angle between Z_{j-1} and Z_j with respect to the rotation around X_{j-1}, d_j is the distance between Z_{j-1} and Z_j along X_{j-1}, θ_j is the angle between X_{j-1} and X_j with respect to the rotation around Z_j, r_j is the distance between X_{j-1} and X_j along Z_j. All limbs and all joint axes of the fully-parallel chains are respectively noted ${}^jC_i$ and $\mathbf{Z_j^i}$ with $j = 1, 2$ indicating the kinematic chain index the frame belongs to and $1 \leq i \leq 9$ as given in Figure 3, where $(A,\ B,\ D,\ E,\ F\ \&\ G)$ are the centers of the links $(C_3^1,\ C_3^2,\ C_4^1,\ C_4^2,\ C_6^1\ \&\ C_6^2)$ respectively. The relative coordinates for these centers with respect to the previous link are defined as $A(X_A^f,\ Y_A^f,\ Z_A^f)$, $B(X_B^f,\ Y_B^f,\ Z_B^f)$, $D(X_D^{3,1},\ 0,\ Z_D^{3,1})$, $E(X_E^{3,2},\ 0,\ Z_E^{3,2})$, $F(X_F^0,\ Y_F^0,\ Z_F^0)$ and $G(X_G^0,\ Y_G^0,\ Z_G^0)$ respectively. Since the new hybrid mechanism is generic,

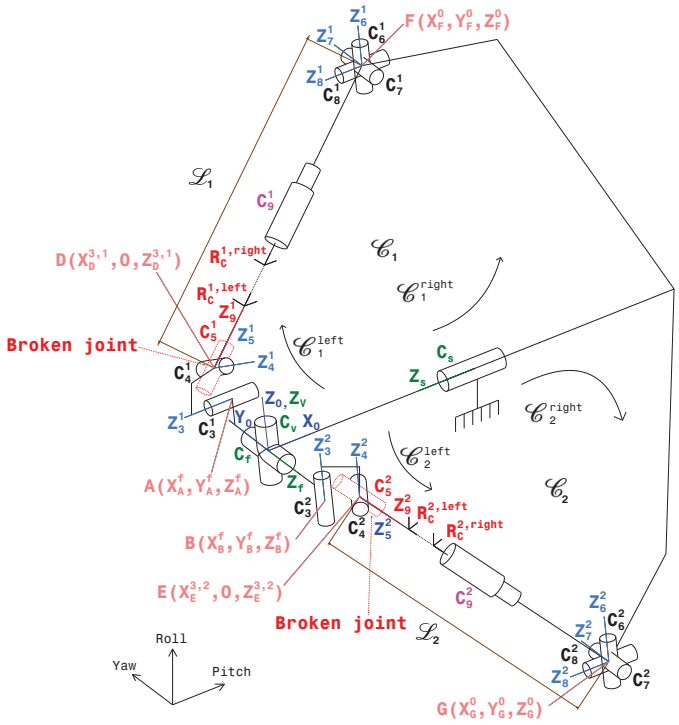

Figure 3: Detailed Kinematic Model for Glenohumeral Shoulder

some parameters have to be set to particular values (see Figure **??** for the definition of these parameters),in order to get the complete description of the hybrid hip solution. These conditions can be summarized in the following set of equations:

$$X_A^f = X_B^f,\ Y_A^f = -Y_B^f,\ Z_A^f = Z_B^f \tag{1}$$

$$X_D^{3,1} = Z_D^{3,1} = X_E^{3,2} = Z_E^{3,2} = 0 \tag{2}$$

$$X_F^0 = X_G^0,\ Y_F^0 = -Y_G^0,\ Z_F^0 = Z_G^0 \tag{3}$$

Once the novel kinematic structure has been proposed, carrying out its performance analysis is required. This analysis will be based on geometrical models that are detailed in the next section.

sectionMODELLING & KINEMATIC ANALYSIS

In order to carry out the kinematic analysis with the help of a simulation tool, two models have to be established. These models concern, first, the Inverse Geometrical Model IGM used to calculate the linear actuator lengths $(\mathcal{L}_j,\ \ j = 1, 2)$ for a given posture of the arm or the leg whenever the shoulder or the

Table 1: Khalil et al. parameters for the generic hybrid mechanism

j	i	σ_j	γ_j	b_j	α_j	d_j	θ_j	r_j
C_v	C_0	0	0	0	0	0	θ_v	0
C_f	C_v	0	0	0	$\frac{\pi}{2}$	0	$-\theta_f - \frac{\pi}{2}$	0
C_3^1	C_f	0	0	0	$\frac{\pi}{2}$	X_A^f	$\theta_3^1 - \theta_3^{1,0}$	$-Y_A^f$
C_4^1	C_3^1	0	0	0	$\frac{\pi}{2}$	$X_D^{3,1}$	$\theta_4^1 + \theta_4^{1,0}$	0
C_5^1	C_4^1	0	0	0	$\frac{\pi}{2}$	0	θ_5^1	0
$R_C^{1,left}$	C_5^1	0	0	0	0	0	0	0
C_6^1	C_0	0	0	0	0	X_F^0	$\theta_6^1 + \pi$	$-Y_F^0$
C_7^1	C_6^1	0	0	0	$\frac{\pi}{2}$	0	$\theta_7^1 + \frac{PI}{2}$	0
C_8^1	C_7^1	0	0	0	$\frac{\pi}{2}$	0	$\theta_8^1 - \theta_8^{1,0}$	0
C_9^1	C_8^1	1	0	0	α_9^1	0	0	$-R_1$
$R_C^{1,right}$	C_9^1	0	0	0	0	0	$-\frac{\pi}{2}$	0
C_3^2	C_f	0	$-\frac{\pi}{2}$	0	$\frac{\pi}{2}$	X_B^f	$\theta_3^2 - \theta_3^{2,0}$	$-Y_B^f$
C_4^2	C_3^2	0	0	0	$\frac{\pi}{2}$	$X_E^{3,2}$	$\theta_4^2 + \theta_4^{2,0}$	0
C_5^2	C_4^2	0	0	0	$\frac{\pi}{2}$	0	θ_5^2	0
$R_C^{2,left}$	C_5^2	0	0	0	0	0	0	0
C_6^2	C_0	0	0	0	0	X_G^0	$\theta_6^2 + \pi$	$-Y_G^0$
C_7^2	C_6^2	0	0	0	$\frac{\pi}{2}$	0	$\theta_7^2 + \frac{\pi}{2}$	0
C_8^2	C_7^2	0	0	0	$\frac{\pi}{2}$	0	$\theta_8^2 + \theta_8^{2,0}$	0
C_9^2	C_8^2	1	0	0	$-\alpha_9^2$	0	0	$-R_2$
$R_C^{2,right}$	C_9^2	0	0	0	0	0	$-\theta_C^2$	0

hip mechanism is considered. The other model concerns the kinematic performance will be presented in the second part of this work.

3.1 Inverse Geometrical Model - IGM

As mentioned above, there are two kinematic closed loops named $\mathcal{C}_j$, depicted in Fig. 3. Each of them is composed of the links ${}^jC_i$ as follows: (C_s, C_v, C_f, C_1^j, C_2^j, C_3^j, C_4^j, C_5^j, C_6^j, C_7^j, C_8^j, C_9^j) with $1 \leq j \leq 2$. The spherical joints that link the linear actuator to the base platform of the fully parallel subpart are split on three independent orthogonal axes (See Fig. 3). The connection of the linear actuator to the moving platform of the fully parallel subpart consists of a universal joint and a rotational one; the former allows the rotational movement of the linear actuator around its own axis and is chosen to be the "broken" joint to establish the IGM of the fully parallel subpart as shown in Figure **??**. The technique of breaking the kinematic closed loops to identify the equivalent kinematic open loop has been used to get the desired IGM. This choice was justified by the need to split the kinematic closed loops into two equivalent halves whenever the number of joints is considered. The upper script $Left$ and $Right$ are added to each closed $\mathcal{C}_j$ to identify the left and the right parts, respectively.

To generalize our model, we take into consideration the fact that the center of the links C_j^i (with $i \in \{1, 2\}$ and $j \in \{3, 4, 6\}$) is variable.

The inputs parameters of the hybrid mechanism are the linear actuator lengths $\mathcal{L}_j$. The outputs are grouped in a three-dimension vector named $\mathbf{q_a} = (q_s, q_v, q_f)^t$. All other i^{th} passive joints of the two closed loops are named θ_i^j where j is the closed loop index. Table 1 gives the required parameters for the description of the two branches of the two closed loop.

To establish the IGM model of the mechanism, the pitch rotation is straight forward since it belongs to the serial part. However, getting the roll and yaw rotations (parallel part) requires eliminating all passive joints angle θ_i^j in the geometrical constraints of closing the kinematic loops $\mathcal{C}_j$.

Hence, the base of the fully parallel mechanism can be considered, without any loss of generalization, to be fixed to link C_1. The target is to establish the relations giving the lengths of actuators function of the elements of vector $\mathbf{q_a}$. Since the closed loops $\mathcal{C}_j$ were broken at the joint $\mathbf{Z}_5^j$ of each, two sub-branches have to be considered. The first one, named left branch, connects links C_4^j to C_v, and the other, named right branch, links the limbs going from C_v^j to C_9^j. The homogenous transformation matrix between the two frames R_0 attached to link C_v and R_5 fixed on C_5^j can be expressed in the two circuits, using either the right or the left sub-branch. The closure loop relation yields the obvious equation between both homogenous matrices ${}^1\mathbf{T}_5^{Right,j}$ and ${}^1\mathbf{T}_5^{Left,j}$:

$$ {}^1\mathbf{T}_5^{Right,j} = {}^1\mathbf{T}_5^{Left,j} \quad 1 \leq j \leq 2 \tag{4}$$

The expressions of the elements of the above matrices are arrived at by multiplying all successive homogenous transformation matrices and using the following notations: $S_k^j = \sin(\theta_k^j)$ and $C_k^j = \cos(\theta_k^j)$. The same notations are used for the sine and cosine functions of α_1, α_2, γ_2 (see table 5 for the definition) and for the vector $\mathbf{q_a}$ elements. To exemplify, the first loop $\mathcal{C}_1$ closing relation (Eq. 4) is detailed below. Using the equivalence between the third and fourth columns of each matrix, we obtain the following relations:

$$(C_3^i)^2 a_{1,k}^i + S_3^i C_3^i a_{2,k}^i + C_3^i a_{3,k}^i + S_3^i a_{4,k}^i + a_{5,k}^i = 0 \tag{5}$$

The way to obtain the above equations (5) and the expression of $a_{j,k}^i$ are detailed in the Appendix for $i \in \{1, 2\}$, $j \in \{1, 2, 3, 4, 5\}$ and $k \in \{1, 2, 3\}$
The equation(5)for k=2 gives:

$$S_3^i = -\frac{(C_3^i)^2 b_1^i + C_3^i b_3^i + b_5^i}{C_3^i b_2^i + b_4^i} \tag{6}$$

by replacing equation (6) with equation (5) for k=1 and k=3, we obtain:

$$(C_3^i)^3 b_{1,n}^i + (C_3^i)^2 b_{2,n}^i + C_3^i b_{3,n}^i + b_{4,n}^i = 0 \tag{7}$$

with

$$b^i_{1,n} = a^i_{1,k}a^i_{2,2} - a^i_{2,k}a^i_{1,2} \quad (8)$$

$$b^i_{2,n} = a^i_{1,k}a^i_{4,2} - a^i_{2,k}a^i_{3,2} + a^i_{3,k}a^i_{2,2} - a^i_{4,k}a^i_{1,2} \quad (9)$$

$$b^i_{3,n} = -a^i_{2,k}a^i_{5,2} + a^i_{3,k}a^i_{4,2} - a^i_{4,k}a^i_{3,2} + a^i_{5,k}a^i_{2,2} \quad (10)$$

$$b^i_{4,n} = -a^i_{4,k}a^i_{5,2} + a^i_{5,k}a^i_{4,2} \quad (11)$$

with $n \in \{1, 2\}$

Combining equation (7) for $n = 1$ and equation (7) for $n = 2$, we obtain a second order polynomial equation in C^i_3

$$L^i_1(C^i_3)^2 + L^i_2C^i_3 + L^i_3 = 0 \quad (12)$$

with

$$L^i_1 = b^i_{1,1}b^i_{1,2} - b^i_{1,2}b^i_{2,1} \quad (13)$$

$$L^i_2 = b^i_{1,1}b^i_{3,2} - b^i_{1,2}b^i_{3,1} \quad (14)$$

$$L^i_3 = b^i_{1,1}b^i_{4,2} - b^i_{1,2}b^i_{4,1} \quad (15)$$

Solving equation (12) when even $\delta = (L^i_2)^2 - 4L^i_1L^i_3 >= 0$, we obtain:

$$\theta^i_3 = \pm \arccos(\frac{-L^i_2 \pm \sqrt{\delta}}{2L^i_1}) \quad (16)$$

if $\delta < 0$ no solution for θ^i_3 and the chains cannot be closed. Meanwhile, equation (16) shows 4 solutions $\theta^i_{3,j}$ for θ^i_3 with $i \in \{1, 2\}$ and $j \in \{1, 2, 3, 4\}$. To choose the right solution $\theta^i_{3,sol}$, we adopted the following design criteria. To prevent the overloading on the link and the interference between the parts, the link C^i_3's rotation should be limited. This yields the following rotation:

$$\theta^i_{3,min} < \theta^i_{3,sol} < \theta^i_{3,max}$$

On the other hand, as $\theta^i_{3,sol}$ is obtained numerically, it should satisfy equations (5). Hence, a numerical error $Err(\theta^i_{3,sol})$ can be established as the sum of the errors induced by each equation: $Err(\theta^1_{3,i}) = \sum_{r=1}^{3} Err^2_{i,r}$.

$$Err_{i,r} = (C^1_{3,i})^2a^i_{1,r} + S^1_{3,i}C^1_{3,i}a^i_{2,r} + C^1_{3,i}a^i_{3,r} + S^1_{3,i}a^i_{4,r} + a^i_{5,r}$$

The used condition for the choice of the appropriate $\theta^i_{3,sol}$ solution can be stated as: $Err(\theta^i_{3,sol}) < \epsilon, \quad i \in \{1, 2\}$. From the forth column of the first member of the closure loop relation for chain 1, and using the value $\theta^1_{3,sol}$, the following can be established:

$$X^0_D = (-C_vS_fC^1_{3,sol} + S_vS^1_{3,sol})X^{3,1}_D - C_vC_fZ^{3,1}_D - C_vS_fX^f_A + C_vC_fY^f_A + S_vZ^f_A \quad (17)$$

$$Y^0_D = (-S_vS_fC^1_{3,sol} - C_vS^1_{3,sol})X^{3,1}_D - S_vC_fZ^{3,1}_D - S_vS_fX^f_A + S_vC_fY^f_A - C_vZ^f_A \quad (18)$$

$$Z^0_D = -C_fC^1_{3,sol}X^{3,1}_D + S_fZ^{3,1}_D - C_fX^f_A - S_fY^f_A \quad (19)$$

Since the center F is fixed, we have the length of the piston of Chain 1:

$$\mathcal{L}_1 = \sqrt{(X^0_D - X^0_F)^2 + (Y^0_D - Y^0_F)^2 + (Z^0_D - Z^0_F)^2} \quad (20)$$

The same calculation for chain 2 leads to the following conditions of point E coordinates:

$$X^0_E = (-C_vC_fC^2_{3,sol} + S_vS^1_{3,sol})X^{3,2}_E + C_vS_fZ^{3,2}_E - C_vS_fX^f_B + C_vC_fY^f_B + S_vZ^f_B \quad (21)$$

$$Y^0_E = (-S_vC_fC^2_{3,sol} - C_vS^2_{3,sol})X^{3,2}_E + S_vS_fZ^{3,2}_E - S_vS_fX^f_B + S_vC_fY^f_B - C_vZ^f_B \quad (22)$$

$$Z^0_E = S_fC^2_{3,sol}X^{3,2}_E + C_fZ^{3,2}_E - C_fX^f_B - S_fY^f_B \quad (23)$$

Since the center G is fixed, we have the length of the piston of Chain 2:

$$\mathcal{L}_2 = \sqrt{(X^0_E - X^0_G)^2 + (Y^0_E - Y^0_G)^2 + (Z^0_E - Z^0_G)^2} \quad (24)$$

In case of hip mechanism, the center of the links C^i_4 is coincident with the center of the links C^i_3. Therefore, the following relations can be written:

$$X^{3,1}_D = X^{3,1}_E = Z^{3,1}_D = Z^{3,1}_E = 0$$

Hence, the new expression of centers D and E coordinates is given in the following set of equations:

$$X^0_D = X^0_A = -C_vS_fX^f_A + C_vC_fY^f_A + S_vZ^f_A \quad (25)$$

$$Y^0_D = Y^0_A = -S_vS_fX^f_A + S_vC_fY^f_A - C_vZ^f_A \quad (26)$$

$$Z^0_D = Z^0_A = -C_fX^f_A - S_fY^f_A \quad (27)$$

$$X^0_E = X^0_B = -C_vS_fX^f_B + C_vC_fY^f_B + S_vZ^f_B \quad (28)$$

$$Y^0_E = Y^0_B = -S_vS_fX^f_B + S_vC_fY^f_B - C_vZ^f_B \quad (29)$$

$$Z^0_E = Z^0_B = -C_fX^f_B - S_fY^f_B \quad (30)$$

To get the IGM of the hip mechanism, the previous values of centers D and F coordinates have to be used in equations (20) and (24). Once the IGM model is established, we present in the next results section how it is used to optimize the proposed solution for the hip and shoulder mechanisms.

4 Optimization

In the early stage of designing a robotic system, it is required to determine the appropriate stress on the mechanical part. The figure 5 presents a kinematic schema for the proposed solution for the roll and yaw motion of the shoulder. The Mechanism are projected on the transverse plan for clarification purposes. Mechanical part 1 in figure5 is taken as an example for the following study. Supposed that the linear actuator are hydraulic cylinder, we can get, for each pressure, the generated force and torque and its influence thanks to the established IGM . For each roll and yaw angle θ_y and θ_z, the IGM provides the new coordinates for the points D and E and then we get the vectors $\vec{FD}$ and $\vec{GE}$ as the point F and G are always fixes. Based on these vectors, the direction of the force produced by the linear actuators become known. $F_{0,0}$, $F_{1,1}$ and $F_{2,2}$ are an example for the produced force for different roll and yaw angle. In addition, The moment vectors $\vec{M}_y$ and $\vec{M}_z$ produced axis will be defined. Each torque is called a quasi-static torque since it is based on the geometrical effects of the lever arm between each linear actuator and the axis of rotation. This is the first step in pre-dimensioning the proposed mechanism that has to be extended to kinetostatic and dynamic analysis in order to manage an external effort applied on the arm. The figure 4 presents the quasi-static torque generated by the 2 linear actuators for each roll and yaw angle. Based on the force and moment acting on the mechanical part, we can get an idea about the stress on this part function of the angle motion.

$$\sigma_i \mapsto f(\theta_{yi}, \theta_{zi}) \tag{31}$$

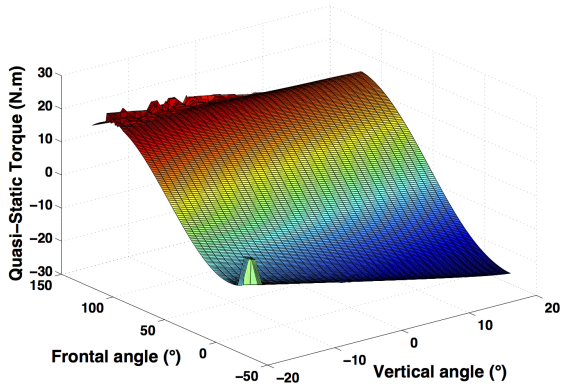

Figure 4: Quasi-static torque function of the yaw and roll angle

The future work will be based on this quasi-static torque provided by the mathematical model of the IGM in order to begin in the phase of mechanical design optimization. This will help the designer to get a tool for obtaining a light weight and optimized structure.

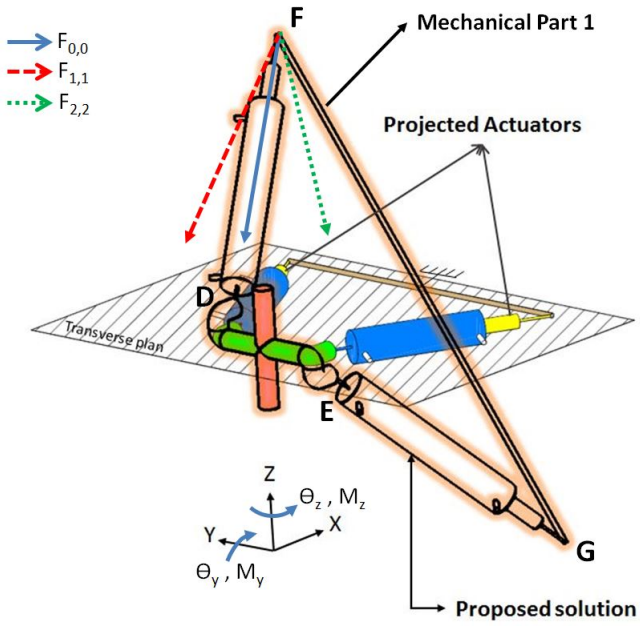

Figure 5: Kinematic schema for the proposed solution for the roll and yaw motion of the shoulder

5 Conclusion

In this paper, we present the kinematic model proposed for the glenohumeral shoulder for HYDROïD robot. We justify our hybrid solution by presented the benefits attained by using both serial and parallel mechanisms. Then, a generic Inverse Geometrical Model (IGM) has been detailed for the hybrid structure to be the first step toward the optimization process. This will be given in the second part of this work.

References:

[1] Kaneko, K., Kanehiro, F., Morisawa, M., Akachi, K., Miyamori, G., Hayashi, A. and Kanehira, N. (2011) Humanoid robot HRP-4 - Humanoid robotics platform with lightweight and slim body, in IEEE International Conference on Intelligent Robots and Systems, pp. 44004407.

[2] Y. Sakagami, R. Watanabe, C. Aoyama, S. Matsunaga, N. Higaki, and K. Fujimura,The intelligent ASIMO: system overview and integration,

IEEE/RSJ International Conference on Intelligent Robots and Systems 3 (2002).

[3] K. Nishiwaki, J. Kuffner, S. Kagami, M. Inaba, and H. Inoue, The experimental humanoid robot H7: a research platform for autonomous behaviour,Philosophical transactions. Series A, Mathe- matical, physical, and engineering sciences 365, 79107 (2007).

[4] W. Khalil and E. Dombre, Modeling, Identification and Control of Robots (2002).

[5] S. Alfayad, A. M. Tayba, F. B. Ouezdou, and F. Namoun, Kinematic Synthesis and Modeling of a Three Degrees-of-Freedom Hybrid Mechanism for Shoulder and Hip Modules of Humanoid Robots, Journal of Mechanisms and Robotics 8 (2016).

[6] S. Alfayad, F. B. Ouezdou, and F. Namoun, New three DOF ankle mechanism for humanoid robotic application: Modeling, design and realization, Journal of Mechanical Design 49694976 (2009).

[7] S. Alfayad, F. B. Ouezdou, F. Namoun, O. Bruneau, and P. He naff, Three DOF hybrid mechanism for humanoid robotic application: Modeling, design and realization, IEEE/RSJ International Conference on Intelligent Robots and Systems, IROS 2009 49554961 (2009).

[8] M. Okada and Y. Nakamura, Development of a cybernetic shoulder-a 3-DOF mechanism that imitates biological shoulder motion, IEEE Transactions on Robotics 21, 438444June (2005).

[9] L. Geppert, Qrio, the robot that could, IEEE Spectrum 41 (2004).

[10] Y. Ogura, H. Aikawa, K. Shimomura, A. Morishima, H.-O. Lim, and A. Takanishi, Development of a new humanoid robot WABIAN-2, Robotics and Automation, 2006. ICRA 2006. Proceedings 2006 IEEE International Conference on, 7681May (2006).

[11] G. Cheng, S. H. Hyon, J. Morimoto, A. Ude, G. Colvin, W. Scroggin, and S. C. Jacobsen, CB: A humanoid research platform for exploring NeuroScience, in Proceedings of the 2006 6th IEEE-RAS International Conference on Humanoid Robots, HUMANOIDS (2006), pp. 182187.

[12] I. a. Murray, Ph.D Thesis, Centre for Rehabilitation and Engineering Studies, University of Newcastle upon Tyne 1470 (1999).

[13] N. Klopcar, M. Tomsic, and J. Lenarcic, A kinematic model of the shoulder complex to evaluate the arm-reachable workspace, Journal of Biomechanics 40, 8691 (2007).

[14] B. Tondu, A kinematic Model of the Upper Limb with a Clavicle-like Link for Humanoid Robots, International Journal of Humanoid Robotics 5, 87118 (2008).

[15] W. Maurel and D. Thalmann, Human shoulder modeling including scapulo-thoracic constraint and joint sinus cones, Computers and Graphics (Pergamon) 24, 203218 (2000).

[16] S. Dayanidhi, M. Orlin, S. Kozin, S. Duff, and A. Karduna, Scapular kinematics during humeral elevation in adults and children, Clinical Biomechanics 20, 600606 (2005).

[17] S. Alfayad, F. B. Ouezdou, F. Namoun, O. Bruneau, and P. Henaff, Three dof hybrid mechanism for hu- manoid robotic application: Modeling, design and realization, in 2009 IEEE/RSJ International Conference on Intelligent Robots and Systems (IEEE, 2009), pp. 49554961.

[18] S. Alfayad, F. B. Ouezdou, F. Namoun, and G. Cheng, High performance Integrated Electro-Hydraulic Actuator for robotics. Part II: Theoretical modelling, simulation, control & comparison with real measurements, Sensors and Actuators A: Physical 169, 124132 (2011).

[19] F. B. Ouezdou, S. Alfayad, P. Pirim, and S. Barthelemy, Humanoid head prototype with uncoupled eyes and vestibular sensors, in 2006 IEEE/RSJ International Conference on Intelligent Robots and Systems (IEEE, 2006), pp. 29802985.